ASC2024-3MOr1B-01

Experimental Validation of a Scaling Law for the Critical Current of Commercial REBCO Tapes as a Function of Magnetic Field and Temperature

G. Succi, A. Ballarino, S. C. Hopkins, Y. Yang

***Abstract*—Much information is lacking at present on the electrical properties of commercial REBCO tapes. This work, which builds on a previous paper of the same authors, presents the results of an experimental campaign aimed at deriving the critical current of tapes from SuperPower, Fujikura, Faraday Factory, and Shanghai Superconductor Technology. The campaign was conducted by applying both the transport method at 4.2 K, in perpendicular background magnetic fields of up to 15 T, and the magnetization method from 4.2 K up to the critical temperature in fields of up to 10 T.**

This latter method was adopted to determining the so-called crossover field, B_0, at which the transition from single vortex pinning to collective pinning takes place. B_0 is challenging to determine by the transport method because of the high currents involved (at 4.2 K, B_0 is roughly 1 T, which corresponds to currents above 1500 A, for a 4 mm tape). Magnetization measurements corroborate transport measurements at 4.2 K both below B_0 and up to 10 T. Further magnetization measurements above 4.2 K allow the temperature dependence of the scaling parameters to be derived, for correlation with the methodology of flux pinning enhancement by different manufacturers. This provides insights about the effectiveness and interplay of pinning mechanisms.

***Index Terms*—Magnetization, Transport measurement, Coated conductors, Pinning, Scaling laws**

I. INTRODUCTION

Coated conductors in the form of tapes made from REBCO ($RE_1Ba_2Cu_3O_{7-\delta}$) superconductor are a game changer in the conception of devices for generating high magnetic fields. Nowadays, commercially available 4 mm wide coated conductors have reached critical current densities J_c(4.2 K, 15 T) = $6 \cdot 10^4$ A/mm^2, which correspond to engineering current densities of about J_{eng}(4.2 K, 15 T) = 1500 A/mm^2 in perpendicular field to the broad face of the conductor, as has been tested for the scope of this work. This even surpasses high-performance Bi-2212 wires reported in [1], [2]. Nonetheless, the design and modelling of coils and other devices wound with REBCO tapes require an accurate knowledge of their electrical properties.

Unlike low-temperature superconductors (LTS), for which the critical current, I_c, is a function of the magnetic field intensity, B, and temperature, T, REBCO displays a dependency of I_c also upon the orientation angle, θ, of the applied magnetic field with respect to the tape. This results from the anisotropic features of the crystalline lattice of REBCO, which induces much better electrical conduction along the *ab*-planes than along the *c*-axis, due to the mass anisotropy.

Furthermore, REBCO coated conductors can include a variety of engineered defects for improving the electrical properties. These can be differentiated into two types. The first type are uncorrelated (random) defects, such as precipitates and point defects, which enhance conduction at all angles. Alternatively, there are correlated defects such as nanorods, twin boundaries and dislocations that enhance the performance at specific angles [3].

Such an intrinsic material complexity is augmented by the manufacturing route, which determines the growth rate of the REBCO layer and the artificial pinning landscape, which in turn impacts considerably on the critical current dependence upon field, temperature, and angle [4]. At present, the design of a device is constrained, basically, to the choice of a single type of tape from a specific manufacturer and it demands for the full characterization of the tape performance over the ranges of interest.

Scaling laws are capable of describing tape performance with much lesser burden compared to a thorough experimental campaign [5]. In a previous work from the authors [6], a comprehensive law for the scaling of the field and temperature dependence of the critical current of REBCO coated conductors has been proposed. It was shown that the law possesses a general character and that it can therefore be adapted to describe the electrical properties of tapes from all manufacturing routes. In [6] it has been successfully applied to a set of experimental data of a tape from one manufacturer, showing the potential in describing the properties across both the field and temperature domains.

This work was supported in part by UKRI STFC under Grant ST/T001844/1 and in part by CERN Doctoral Student Programme.

G. Succi is with the European Organization for Nuclear Research (CERN) 1211 Geneva, Switzerland, and with the Faculty of Engineering and Physical Sciences, University of Southampton, SO17 1BJ Southampton, U. K. (email: giovanni.succi@cern.ch).

A. Ballarino and S. C. Hopkins are with CERN, 1211 Geneva, Switzerland.

Y. Yang is with the Institute of Cryogenics, Faculty of Engineering and Physical Sciences, University of Southampton, SO17 1BJ Southampton, U.K.

The present work extends the results to four tape samples from four manufacturers: SuperPower (SP), Fujikura, Shanghai Superconductor Technology (SST), and Faraday Factory Japan (FFJ), with the aim to validate the scaling law over a wide magnetic field range, spanning from a few milliteslas up to the irreversibility field, B_{irr}, and temperature range, namely from 4.2 K up to the critical temperature, T_c.

In the experimental campaign, a field of up to 15 T is applied perpendicular to the broad face of the REBCO tapes and the transport I_c is measured at 4.2 K. Magnetization measurements were also conducted by exposing tape samples to a perpendicular field and recording the magnetization cycle from 4.2 K up to T_c in magnetic fields of up to 10 T.

A relevant topic discussed in this work is the temperature dependence of the scaling parameters and the correlation with the involved pinning mechanisms of each manufacturer.

II. The Scaling law

In this section, we recall the scaling law introduced in [6] and the reasons for expressing it in such a way. The mathematical description given for the I_c dependence on field of REBCO tapes is:

$$I_c(B,T^*,\theta^*) = I^*_{c,0} \cdot \left(1+\frac{B}{B^*_0}\right)^{-\alpha^*} \cdot \left(1-\frac{B}{B^*_{irr}}\right)^{q^*} \qquad (1)$$

which is defined for a generic temperature T^* and orientation of the external field, θ^*. The angle is defined relative to the *c*-axis of the crystallographic structure.

Let us note that each parameter in Eq. (1) depends on the temperature and/or the angle. To begin with, $I^*_{c,0} = I_c(T^*, B{=}0)$ regardless of the angle. $B^*_0 = B_0(T^*,\theta^*)$ is a function of both the temperature and the angle, and similarly for the remaining parameters in the formula, α^*, B^*_{irr}, and q^*.

It is important to remark that Eq. (1) has been obtained by modifying the Kramer expression [7], [8], therefore it is based on the physics of pinning and it maintains the correct physical dimensions. For the detailed explanation of the derivation of Eq. (1) and its physical meaning, we refer the reader to [6].

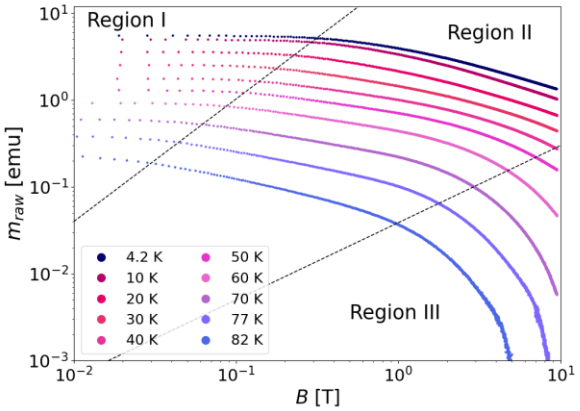

Fig. 1. Magnetic moment of an SST tape tested for the scope of this work. Three regions can be identified, each corresponding to a different pinning regime.

Eq. (1) is structured into three terms. Each of the terms describes a different region of the field dependence of I_c when looking at a double logarithmic plot. As an example, Fig. 1 reports the data of the testing of a tape from SST. The plot shows the magnetic moment, which is directly proportional to the I_c, therefore only the absolute values differ. We come back to the derivation of the currents from the magnetic moment later in Section IV.

Region I features a constant value of the critical current near zero field, which depends on the temperature. At the microscopic level, this is the result of flux vortices being much lower in density than the pinning centers [7]. It is called the 'single vortex' pinning regime and it occurs in the range from 10^{-3} T to 10^{-1} T, but it stretches up to ~ 0.3 T at 4.2 K.

As the applied field exceeds such values, the density of vortices increases at a point that they start interacting and acting collectively. The curve enters *Region II*, marked by the presence of the 'crossover' or 'kink' field, B_0, and by the following linear dependence (in the log-log plot) given by the α exponent. The knowledge of the transition between these two pinning regimes is crucial for applications, therefore our goal is to determine B_0 as a function of temperature. Emphasis has been put in this work into assessing the crossover field from 4.2 K up to close to T_c.

Measuring B_0 is quite challenging. In the transport current method, conducted exclusively in liquid helium at 4.2 K, B_0 is roughly 1 T, which corresponds to I_c above 1500 A for a 4 mm wide tape. Reaching such high currents complicates the measurement set-up. The magnetization method allows us to measure at other temperature levels. However, B_0 is of the order of a few tens of milliteslas above 70 K, therefore acquiring sufficient data points at such low field levels demands precise measurements. This is explained in detail in Section IV.

The last term in Eq. (1) describes the further drop in performance occurring when approaching the irreversibility field, B_{irr}, the limit of application of HTS. It is called the thermal activation regime, since thermal fluctuations are particularly effective in de-pinning the weak pinning centers starting from 30 K – 40 K. The exponent q governs the rapidity of the drop in this *Region III* of the curve.

III. Experimental methods

We employed two different experimental methods to investigate the electrical properties of REBCO tapes. The first method consists in injecting a transport current in a tape immersed in a liquid helium bath at 4.2 K and exposed to background magnetic fields of up to 15 T, perpendicular to the broad face of the tape. The second method relies on a Vibrating Sample Magnetometer (VSM) and measures the

Fig. 2. Left: Inner 1.5 mm groove with six transversal holes for improving the cooling between the tape and the liquid helium. These are inside a 4.5 mm wide groove hosting the tape. Right: VSM sample mounted on its holder and embedded in g-varnish.

magnetic moment of tapes which oscillate rapidly inside a slowly ramping background magnetic field.

It is an objective of this work to establish a correlation between these two methods. By checking that the same field dependence is measured at 4.2 K with both, the transport method is useful to establish the absolute value of the I_c(4.2 K) at zero applied field to scale the curves obtained at the other temperature levels by the magnetization method. Eventually, this enables the temperature dependence of the scaling parameters to be determined for each tape, which is fundamental for the full description of Eq. (1).

The basic features of our experimental set-ups are described in the following. For the transport method, we used a solenoid test station available in the superconductor laboratory at CERN, which generates a background magnetic field to the sample of up to 15 T and which is capable of injecting up to 3 kA in the samples. We developed a sample holder with a 'U' shape to create a short straight region (roughly 15 mm long) where the field is perpendicular to the tape in the magnet bore.

The design implemented an inner 1.5 mm groove and six transversal holes into an already existing 4.5 mm groove that hosts the tape, to improve the heat exchange between the tape and the liquid helium. This has been the essential feature to surpass the barrier of 2000 A injected in the sample, that was particularly limiting during the early stages of the work. Tapes were always tested as produced and no copper shunt was included in parallel to them. Fig. 2 on the left is a closeup of the mentioned inner groove in the central G10 piece.

For the magnetization method, short samples of 4 mm length and 4 mm width were cut and mounted on a small cylindrical sample holder, see Fig. 2 on the right. Let us note that the reversible region was observed in these measurements at high temperatures, typically 77 K and 82 K.

IV. MEASUREMENT RESULTS

A. *Transport current*

The first part of this section is dedicated to the presentation of data from the transport current measurements and to the fitting of such data by means of the scaling law. To begin with, Fig. 3 shows the data of tape samples from three different manufacturers: SuperPower AP (in blue), Shanghai Superconductor Technology ST1910-19 (in green), and

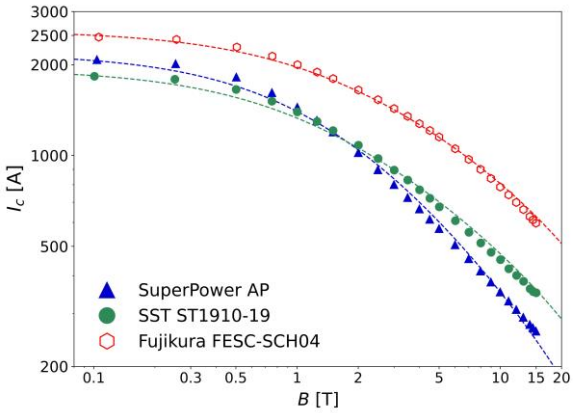

Fig. 3. Transport data of three tapes from different manufacturers, all tested at 4.2 K and down to 0.1 T background field. The tapes are 4 mm wide. The magnetic field is perpendicular to the tapes. Scale is log-log.

Fujikura FESC-SCH04 (in red). The 1 μV/cm criterion is used to determine the critical currents. Data are complemented with the fitting by the scaling law, Eq. (1), represented by dashed lines.

The availability of I_c data down to 0.1 T applied field is of great relevance for fitting using the scaling law as it allows the intercept, $I_{c,0}$, and the crossover field, B_0, to be derived precisely. This is extremely valuable for scaling the data of other tape samples from the same manufacturers, obtained with similar methods (e.g. with the same pinning structure). This information is often lacking at intermediate fields. Table 1 reports the resulting fitting parameters for each of the three curves as well as for a fourth curve shown in Fig. 4. Let us note that q and B_{irr} have been set to 2.0 and 150 T, respectively. B_{irr} was limited to 150 T because of some past estimates on the upper critical field, $B_{c,2}$ on cuprates [9], [10].

The slope q was set between 2, to match the exponent in Kramer's law, and 5 to allow an even faster performance drop in *Region III*. The $I_{c,0}$ in Table 1 varies quite substantially among the different tapes. However, most of the interest here is on the slope of the linear region, α, and on the crossover field, B_0.

B_0 is related to the so-called matching field, B_ϕ, which is determined by $n \cdot \phi_0$, n being the density of the pinning centres in the superconducting layer, and ϕ_0 the flux quantum. In Table 1, B_0 is in the range from 0.84 T to 1.42 T.

A relative variability is observed also on the slope of the linear region. Let us note that this is positive and must be lower than 1.0 because of the physics of pinning (Kramer's

TABLE 1. Resulting scaling parameters for the curves in Fig. 3 and Fig. 4.

Manufacturer	$I_{c,0}$ [A]	α	B_0 [T]
Shanghai ST	1933	0.54	1.06
SuperPower	2182	0.81	1.42
Fujikura	2565	0.50	1.39
Faraday FJ	3904	0.66	0.84

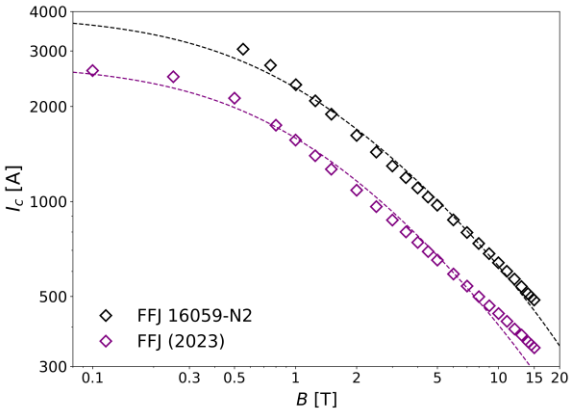

Fig. 4. Transport data of the FFJ tape (in black), tested at 4.2 K down to 0.55 T background perpendicular field, as it reached the 3000 A limit of the power supply. The tape is 4 mm wide.

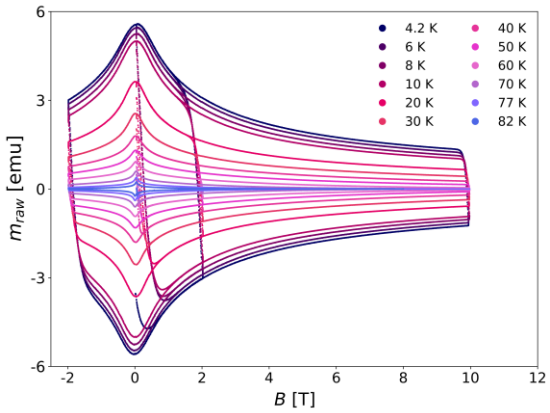

Fig. 5. Magnetic cycles from 4.2 K up to 82 K, for the same SST tape shown in Fig. 3. The field is applied perpendicular to the sample.

law). It resulted to be as low as 0.5 for the Fujikura tape and up to 0.81 for the SuperPower tape. The difference in slope is evident from the crossing between the SuperPower and SST tapes in Fig. 3. Although SuperPower starts from a higher $I_{c,0}$, its α is considerably higher than SST, therefore its performance drops faster. The crossing occurs at roughly 1 T and the performance ends up being considerably higher for the SST tape above 5 T.

The engineering critical current density of the Fujikura tape is J_{eng}(4.2 K, 15 T) = 1500 A/mm^2 and J_{eng}(4.2 K, 5 T) = 2850 A/mm^2 which is higher than the Bi-2212 wires developed in the past years [1], [2].

The case of the FFJ tape is now analysed separately. This tape has also been tested successfully in our solenoidal facility. However, it reached the current limit of the power supply, which is of 3000 A. The beginning of transition was observed at such current level down to 0.55 T applied field, and the I_c was extrapolated to be 3040 A. Fig. 4 shows the result of the testing, where data for this tape are represented in black. The scaling is challenging, as insufficient data are available in the relevant region below 0.5 T, where the second term in Eq. (1) plays the most important role.

To estimate $I_{c,0}$, we used the data of a similar tape from the same manufacturer tested last year, see the dataset in purple in Fig. 4. The $I_{c,0}$ of this tape was 1.25 times higher than the measured I_c(0.5 T). Consequently, the same factor was applied to the recent tape. The resulting fitting applying the scaling law in Eq. (1) is reported by the dashed line. The scaling is 8.8% lower than the datapoints at 0.55 T, 4.5 % higher at 2 T, and 7.4% lower at 15 T. Data of the older tape were also fitted, see the dashed line in purple.

B. Magnetic moment

In the Vibrating Sample Magnetometer technique, a small sample (typically 4 mm wide and 4 mm long) is oscillated inside a background field imposed by a solenoid magnet. The frequency of oscillation is 20.4 Hz and the field ramp rate is typically between 100 – 300 mT/min, such that the sample experiences a quasi-static field during a single oscillation. Fig. 5 shows the magnetic cycles for the same SST tape tested by the transport method and shown in Fig. 3. Cycles were recorded at 4.2 K, 6 K, 8 K, 10 K, 20 K, 30 K, 40 K, 50 K, 60 K, 70 K, 77 K, and 82 K. The magnetic moment is expressed in emu. As mentioned already, the field in a typical measurement is raised from zero up to 10 T, lowered to -2 T, then increased again to 2 T, and finally reduced to zero. This allows verification of the overlap of data in the initial part of the direct branch. Thus, this confirms the proper running of the measurement (e.g. temperature stability) while saving precious time with respect to conducting a full magnetic cycle.

The scaling law is applied to the reversal (upper) branch of the cycle, since this branch is recorded continuously from the beginning to end. Moreover, the reversal branch is perfectly symmetric to the direct (lower) branch. The absolute values of the current are derived by dividing the curves by the peak magnetic moment at 4.2 K, $m_{peak,4K}$, and multiplying by the I_c(4.2 K, 0.1 T) obtained by the transport current method. The utility of these curves lies especially in deriving the parameters of the scaling law, Eq. (1). Fig. 6 shows the

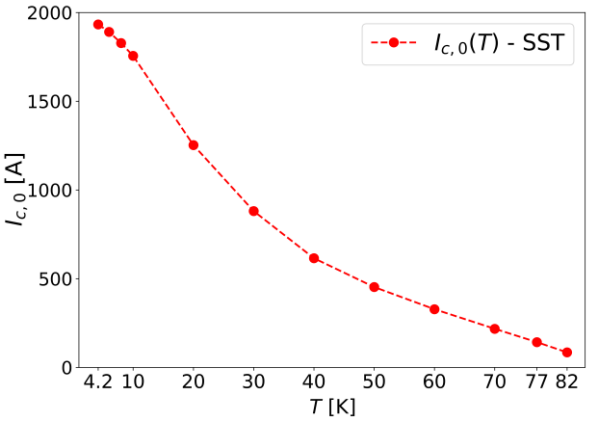

Fig. 6. Intercept $I_{c,0}$ for the SST tape as a function of temperature.

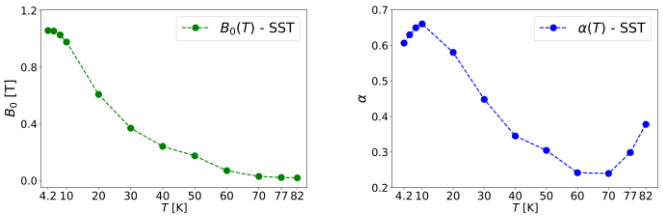

Fig. 7. Crossover field (left) and slope of the linear region (right) for the SST tape as a function of temperature.

resulting temperature dependence of $I_{c,0}$ for the SST tape, where the starting value at 4.2 K is the same reported in Table 1, namely 1933 A. The region below 10 K is of particular interest, since the concavity of the curve is different from the region above 10 K. To further investigate on this, we refined the measurements in the low temperature region, namely at 4.2 K, 6 K, 8 K, and 10 K for the other tapes tested in this work as well.

Fig. 7 presents the temperature dependence of B_0 and α. The crossover field starts from 1.06 T and, after following a plateau-like region at low temperatures, it decreases gently with increasing temperature. Conversely, the slope of the linear region starts from 0.61 at 4.2 K, it goes up until 10 K reaching 0.66, then drops progressively to 0.24 at 60 K, and it increases finally to 0.37 at 82 K. This is an indication that different pinning mechanisms might intervene at different temperatures.

Fig. 8 shows the temperature dependence also of the last two scaling parameters, B_{irr} and q. B_{irr} starts from 150 T at 4.2 K and it remains so up to 20 K before it decreases. While we keep such constant value in this temperature range for the scope of this work, we are aware that it is not physically realistic, and we are currently working on analytical formulations to describe a smoother temperature variation.

Instead, q stays at the value of 2 up to 30 K, then it jumps to 5 at 50 K, with an intermediate step of 3.64, at 40 K. The shift is because the drop in performance is much more rapid at middle-high temperatures than at low temperatures.

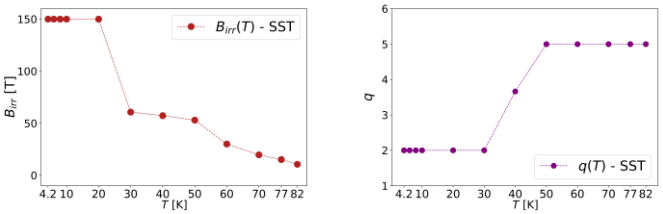

Fig. 8. Irreversibility field (left) and q slope (right) for the SST tape as a function of temperature.

V. Extension of Results and Discussion

The results of the testing of another three tapes are reported in this section. The methodology to compare the results of the transport and magnetization methods is presented. The temperature dependence of the scaling parameters is derived for all tapes. The statistics on the tapes measured by the transport method is discussed. Finally, B_0 is assessed by precision measurements conducted at high temperatures and at very low magnetic field ramp rates.

A. Methodology: transport versus magnetization

Fig. 9 proposes a comparison between the transport and magnetization data for the Fujikura tape at 4.2 K (shown also previously in Fig. 3). Remarkably, the plot is filled with data down to 0.1 T for both methods. To compare the two sets, the latter have been scaled dividing by the peak magnetization, $m_{peak,4K}$, and multiplying by I_c(4.2 K, 0.1 T) = 2467 A, as indicated in section IV B.

The two curves match up to a high degree over the entire magnetic field range from 100 mT to 10 T. Consequently, a single scaling is adopted for both, which is represented by the black dashed curve. The scaling parameters are those reported in Table 1: $I_{c,0}$ =2565 A, α=0.5, B_0 =1.39 T, while q and B_{irr} are kept at the values described in the previous section at this temperature level, 2.0 and 150 T, respectively. While the difference between the two experimental datasets remains within 2 - 3%, the discrepancy to the scaling curve is up to 5%, observed at 0.5 T.

We highlight that both I_c datasets are plotted as a function of the applied background field. At present, the tape self-field is included in both datasets. The self-field is not uniformly distributed across the tape width [11]. However, the most relevant impact of the self-field is expected to occur below 0.5 T, where the currents are the highest, but the field dependence fades. Curves in Fig. 9 suggest also that the self-field might be similar for both datasets, allowing for a fair comparison between the two.

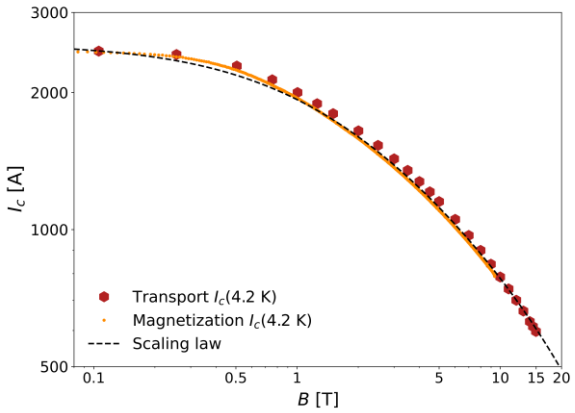

Fig. 9. Transport versus magnetization data (scaled) for the Fujikura tape, at 4.2 K and in perpendicular field.

B. Temperature dependence of the scaling parameters

Fig. 10 - 13 show the scaling parameters of the tapes presented in Section IV. Magnetization measurements on the SP and FFJ tapes were conducted at the University of Geneva. Fig. 10 is for the $I_{c,0}$: as previously mentioned, curves of the magnetic moment at each temperature level are scaled dividing by $m_{peak,4K}$ and multiplying by the I_c(4.2 K, 0.1 T) obtained by the transport method.

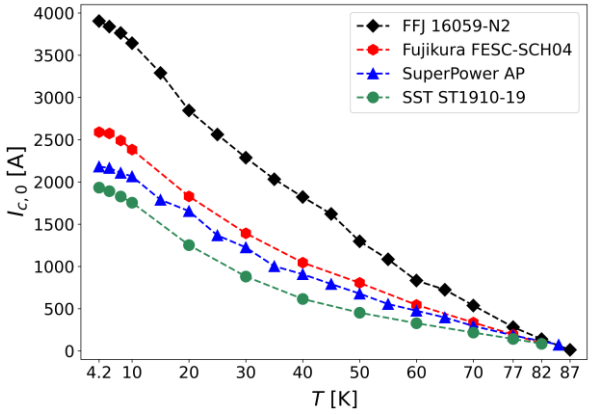

Fig. 10. Critical current at zero background field from 4.2 K up to 87 K, for the same tapes tested by the transport method in Section IV. Values are scaled by I_c(4.2 K, 0.1 T).

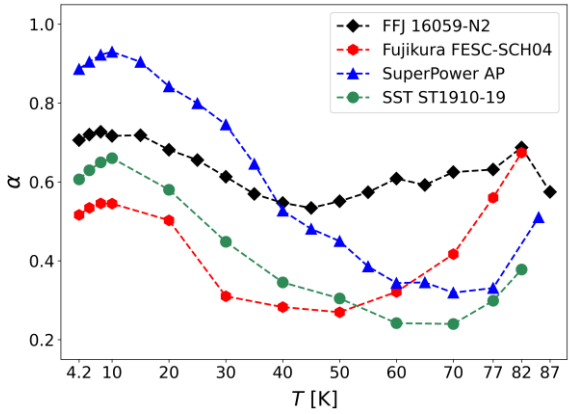

Fig. 11. Slope of the linear region from 4.2 K up to 87 K, for the same tapes tested by the transport method in Section IV.

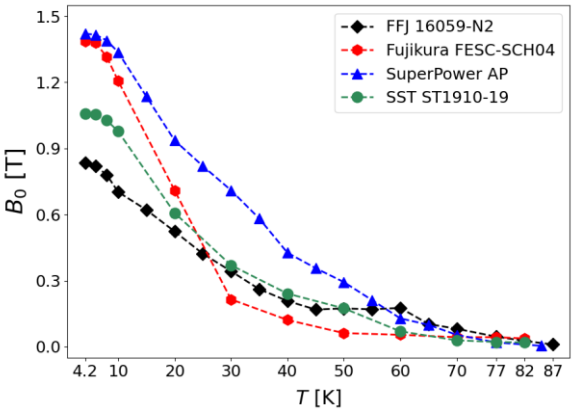

Fig. 12. Crossover field from 4.2 K up to 87 K for the same tapes tested by the transport method in Section IV.

The FFJ tape has much higher performance than the other three tapes. The distinctive feature of the SuperPower AP tape is the relatively slow decrease of the $I_{c,0}$ between 4.2 K and 10 K. The other tapes, instead, tend to experience a faster initial drop. In general, the region below 10 K is of great interest, since the concavity of the curve is different from the region above 10 K. Such behaviour confirms what was observed already in [6], which is unexpected from the theoretical standpoint. The rest of the temperature domain, from 10 K up to 82 K (85 K for SP, 87 K for FFJ) is defined by a mild slope in all cases.

Table 2 sums up much information about the tapes and we refer to it diffusely in the following. First, it is worth commenting on α and B_0 together. Noticeably, the FFJ tape (in black) displays a local maximum of both scaling parameters at 60 K, see Fig. 11 and Fig. 12. We interpret this as a strong pinning effect occurring between 50 K and 60 K, which makes this tape particularly suitable for applications in this range. A higher B_0 means a delayed performance drop, which is relevant for high-temperature applications where the fields involved are contained below a few teslas at most. However, this tape might also be employed at all temperatures, see Table 2, thanks to the remarkable $I_{c,0}$ values.

TABLE II. Manufacturing route, REBCO layer, types of pinning centers, scaling parameters, and inferred application range of the tapes tested for the scope of this work.

Manufacturer	SP	SST	Fujikura	**FFJ**
Route	IBAD+MOCVD	IBAD+PLD	IBAD+PLD	IBAD+PLD
SC layer	(Y,Gd)BCO	GdBCO	EuBCO	YBCO
Pinning	BZO nanorods	No APC	BHO nanorods	Y_2O_3 nanop.
α (<10 K)	0.87 - 0.93	0.61 - 0.66	0.52 - 0.55	0.71 - 0.73
α (>60 K)	0.32 - 0.51	0.24 - 0.38	0.32 - 0.67	0.57 - 0.69
B_0 (<10 K) [T]	1.34 - 1.42	0.98 - 1.06	1.21 - 1.39	0.70 - 0.84
Appl. range	Above 60 K	Overall	Below 60 K	Overall

In fact, Y_2O_3 nanoparticles [12] act as effective pinning centres over a wide range of temperatures, as explained in [4].

The Fujikura tape (in red) behaves differently. α values are comprised between 0.52 - 0.55 below 10 K, which are the lowest among all tapes, while B_0 stays above 1.2 T. In comparison, the SST tape (in green) has slightly higher α, between 0.61 – 0.66, and lower B_0= 0.98 T – 1.06 T in the same temperature range. The combination of α and B_0 keeps the performance of these two tapes very close to each other, and they are preferable for low to middle temperature applications, indicatively below 60 K.

The B_0 of the Fujikura tape drops rapidly below 300 mT already at 30 K and then gently reduces to zero approaching T_c, see Fig. 12. In contrast, the α raises to high values close to T_c (it is 0.67 at 82 K), see Fig. 11. This is the sign that a different pinning mechanism kicks in from middle to high temperatures and it might be interpreted by means of the BHO nanorods indicated in Table 2.

The SST tape undergoes a similar trend in terms of α, however the values are quite low over the entire temperature domain. This makes this tape suitable also in the rest of the temperature domain, namely above 60 K. Instead, B_0 decreases gently with increasing temperature. A single pinning

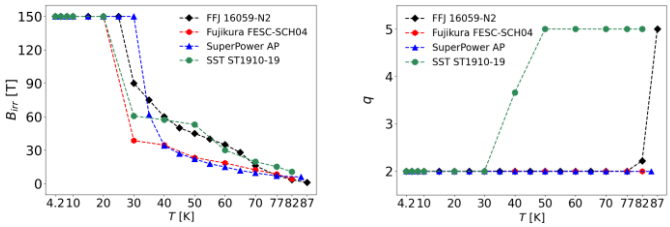

Fig. 13. B_{irr} (left) and q slope (right) for the tapes tested by the transport method in Section IV.

mechanism might be involved in this case, which cannot be attributed to advanced pinning centres (marked as 'No APC' in Table 2), but rather to stacking faults, as it was shown in [13]. The SP tape (in blue) starts from some high values of α, between 0.87 – 0.93, as well as of B_0 = 1.34 T - 1.42 T below 10 K. Then, the latter decreases smoothly with increasing temperature, similarly to the SST tape. The presence of BZO nanorods in the superconducting layer may be at the origin of this behaviour [14]. This mechanism fades gradually as the temperature rises. For such reasons, the SP tape is best suited for applications above 60 K, as the combination of α and B_0 is competitive with SST in this temperature range.

A common feature observed for SST, SP, and Fujikura tapes is that the slope of the linear region raises at high temperatures, having slightly different onsets starting at 50 K - 60 K, see Fig. 11. This might be attributed to creep, which becomes increasingly important at high temperatures, as discussed in Section V D.

For completeness, Fig. 13 sums up the dependence of the irreversibility field, B_{irr}, and of the associated slope of the third term in Eq. (1), q, with temperature. The two plots suggest that the SuperPower and Fujikura tapes have similar phenomenology. In fact, they share a common trend of B_{irr} from 40 K onwards. In addition, the q slope stays to 2 all over the temperature range for both. On the other hand, FFJ and SST tapes might belong to a second category, given the similar higher values of B_{irr} from 40 K onwards. The next step of our work will be to elaborate analytical expressions for the temperature evolution of these parameters, which will allow further understanding of their mutual interplay.

C. Statistics on tape performance

Multiple tape samples have been tested for each of the tapes shown in Fig. 3 and Fig. 4. They were not necessarily the best ones of their respective batches, while rather those tested successfully up to high current levels, typically 2000 A or higher and low applied fields, which is relevant to apply the scaling law.

Fig. 14 displays the performance of four tape samples from the SuperPower AP tape. Critical current tests generally start at the highest available field of 15 T and the field is lowered progressively reaching higher I_c. In three cases (sample no. 1, 2, and 4), tapes were tested down to 0.1 T background field. Sample no. 3 had similar performance to the others, however a sudden degradation occurred at 1 T, forcing the test to be stopped. The degradation came from the central region of the holder, where the tape is exposed to the perpendicular field.

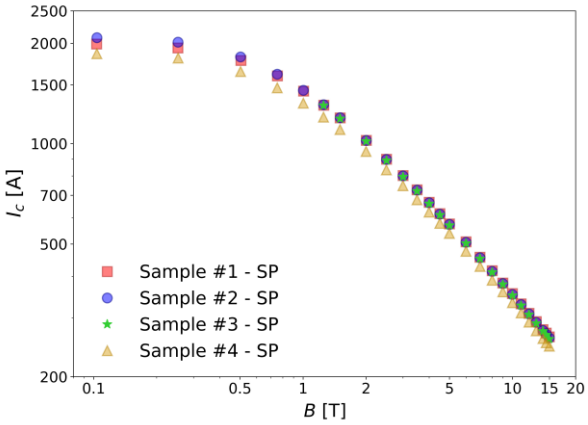

Fig. 14. Statistics on the performance of tape SuperPower AP. The tape is 4 mm wide. Measurements are at 4.2 K and in perpendicular field.

The maximum difference in performance was between samples no. 2 and no. 4 (in blue and yellow in Fig. 14). This was by 5.6 % at 15 T (247.1 A versus 261.7 A), 6.0% at 5 T, and it increased up to 10.4% at 0.1 T (1861 A versus 2078 A). The typical length of a tape sample is 0.4 m and all four tested samples were extracted consecutively from the same spool. It is also relevant to examine the scaling of these curves, to check for correlations between the parameters. This is shown in Fig. 15, where two approaches were tried out. The first one consisted in a 'free' scaling, resulting in α in the range 0.83 – 0.89 for all the four curves. In the second one, instead, the same α was set to 0.81, see Table 1, for all curves (corresponding to sample no. 2 in Fig. 14). Both approaches reveal the hint of an inverse relationship between the B_0 and the intercept, $I_{c,0}$. This result suggests that slightly lowering the density of artificial pinning centers might be helpful to improve the zero field performance of tapes at low temperatures.

Fig. 16 shows the statistics of the FFJ and SST tapes together. Three different samples of the FFJ tape (type N2) were tested. Their performance was less than 1% apart which made it the most consistent tape tested in the campaign. Sample no. 1 is the same already presented in Fig. 4. Sample no. 2 had the same performance down to low fields; in particular, for this test, an early beginning of transition was

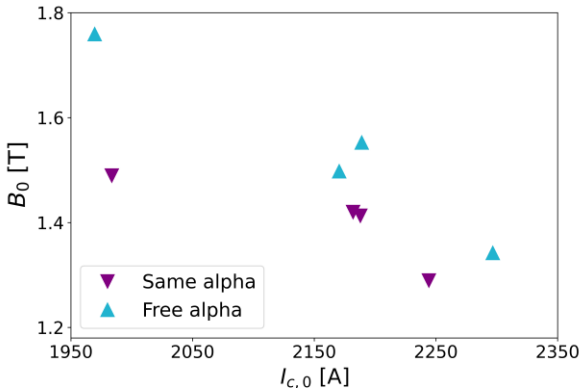

Fig. 15. Effect of having the same or different (free) α on the B_0 as a function of $I_{c,0}$.

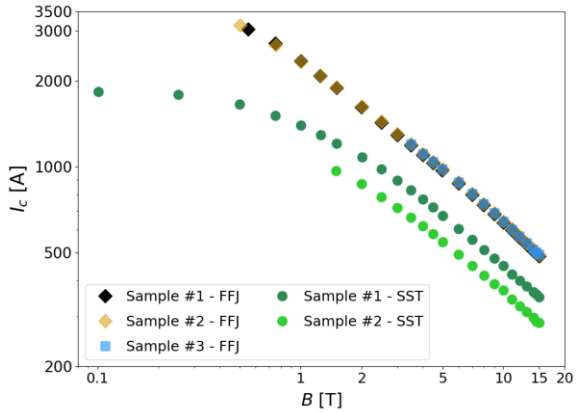

Fig. 16. Statistics on the performance of FFJ and SST tapes. The tapes are 4 mm wide. Measurements are at 4.2 K and in perpendicular field.

observed even down to 0.5 T background field, giving an extrapolated I_c(0.5 T) = 3130 A. Sample no. 3 had a comparable performance to the previous two, however an abrupt degradation was observed at 3.5 T, which is why the data (in light blue) stops there.

The SST tape was tested two times. Sample no. 1 is the same reported in Fig. 3, whereas no. 2 was extracted just adjacent to no. 1 on the same spool. The performance was lower by 18.5% at 15 T (350.2 A versus 285.3 A), which worsened to 19.2% at 5 T (675.7 A versus 546.1 A), and further to 19.9% at 1.5 T (1210 A versus 969.8 A). No data is available below 1.5 T for sample no. 2, as an abrupt degradation occurred in one of the bent regions of the sample.

Fig. 17 shows the results of the tests on four different tape samples for Fujikura FESC-SCH04. Sample no. 1 is the same shown in Fig. 3. Sample no. 2 was also measured down to 0.1 T background field. However, this sample had roughly 36% lower performance (at 0.1 T, 1567 A vs 2467 A), which is quite remarkable considering that it was extracted just next to no. 1. Fig. 17 displays the results of two other samples. Sample no. 3, was measured down to 0.3 T background field, then the sample burnt over one of the bent regions. The testing of sample no. 4, instead, was interrupted at 3 T because of a sudden performance degradation, which occurred from one field level to another. Four additional samples have been tested from the same spool, giving profiles in the same interval defined by those shown here.

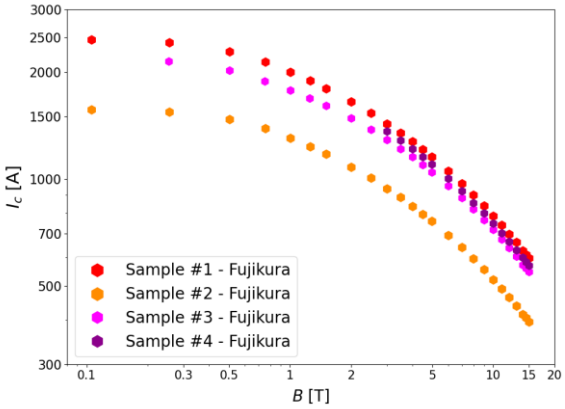

Fig. 17. Statistics on the performance of the Fujikura tape. The tapes are 4 mm wide. Measurements are at 4.2 K and in perpendicular field.

D. Precision measurements on the crossover field, B_0

One relevant investigation of this study is the refinement of the magnetization measurements at high temperatures. The crossover field is below 100 mT above 70 K, as can be grasped from Fig. 12. The ramp rate adopted in the standard magnetization measurements is usually between 100 and 120 mT/min at such temperatures. Considering a typical sampling rate of 2 to 3 seconds for our system, few datapoints could be collected below B_0. This reduces the ability to derive the parameter with good precision, therefore measurements were repeated at ramp rates of 10 mT/min at 70 K and 77 K, and of 5 mT/min at 82 K.

The slower cycles were recorded from zero field with 300 mT and -200 mT reversal fields, namely on a much-shortened cycle with respect to the standard one, since determining B_0 only requires entering the first part of *Region II*. Also, this limits the measurement time to a few hours.

Fig. 18 shows a closeup of the measurement at 82 K, below 0.3 T background field. Magnetization data have been scaled according to the procedure described in section IV B to obtain the displayed I_c. The curve associated to the slow ramp rate has lower peak, while higher slope of the linear region and crossover field. In fact, the slope passes from α_{fast}=0.38 to α_{slow}=0.52, whereas the crossover field goes from $B_{0,fast}$=19 mT to $B_{0,slow}$=31 mT. Table 3 sums up the change in the scaling parameters with the refinement, at 70 K, 77 K, and 82 K, where 100 – 120 mT/min and 5 – 10 mT/min are the fast and slow ramp rates, respectively.

First, a lower dB/dt induces a lower voltage, which translates into a lower magnetic moment, and therefore a lower derived I_c, see the lower peak values of the red curve compared to the blue curve in Fig. 18. Flux creep can be identified as the main cause of the differences in the rest of the observed phenomenology, as it influences the onset and subsequent evolution of the linear region. We suggest that slow ramp rates enable additional defects to act as effective

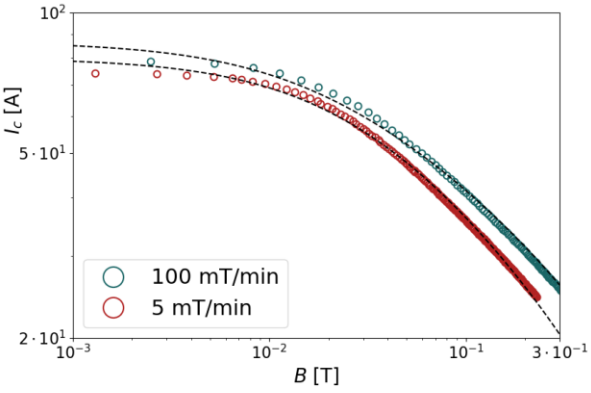

Fig. 18. Refinement of the B_0 measurement at 82 K for the SST tape, conducted at 5 mT/min. The fitting applying the scaling law is shown by the dashed black lines.

TABLE III. Change in the scaling parameters α and B_0 in the measurements from fast to slow ramp rates, at 70 K, 77 K, and 82 K.

T [K]	dB/dt [mT/min]	α	B_0 [mT]
70	120	0.24	29
	10	0.55	142
77	120	0.30	22
	10	0.51	66
82	100	0.38	19
	5	0.52	31

pinning centres. The result is higher B_0, as from the values in Table 3.

It is known that the *n*-value tends to decrease with increasing field, as shown in [6]. A lower dB/dt gives even lower *n*-values with increasing field. This enhances the effect of creep and results in a higher field dependence of the I_c, meaning higher α, as again observed in the values in Table 3.

CONCLUSION

This paper presents the results of an experimental campaign for testing commercial REBCO tapes from four different manufacturers. Critical current tests have been conducted by direct and indirect methods. The direct method is the transport current, which is conducted by means of a so-called U-shape sample holder. This holder exposes the broad face of the tapes, at 4.2 K, to perpendicular fields, in the bore of a solenoid facility that generates up to 15 T. The indirect method measures the magnetic moment of a sample oscillating in a vibrating sample magnetometer at different temperatures and in external perpendicular fields of up to 10 T.

The ultimate scope of the work is to apply the proposed scaling law to the measured data and derive the scaling parameters for each tape manufacturer. Transport data at 4.2 K allow the absolute value of the critical current at zero applied field to be determined. Matching between transport and magnetization data at 4.2 K was verified for all tapes. The magnetization method enables measurements at multiple temperature levels, up to T_c, and it is used to infer the temperature evolution of the scaling parameters for the four tapes from SuperPower, Shanghai Superconductor Technology, Fujikura, and Faraday Factory Japan. Similar patterns have been identified among these tapes and a correlation with the respective pinning mechanisms has been discussed.

Homogeneity in critical current of the tapes has been studied. The findings show that the I_c(4.2 K) is subjected to variations along the spool length in the range up to even 36%.

Specific attention has been dedicated to the detailed measurement of the magnetization at temperatures above 70 K. At such temperatures, the crossover field, B_0, is in the order of a few tens of milliteslas, which made it difficult to measure because of the limited sampling rate of the test station. Consequently, another set of measurements has been conducted at slower ramp rate. New values for the crossover field and the slope of the linear region have been derived, which are consistently higher than the initial values obtained with a faster ramp rate. The involved phenomenology can be qualitatively explained by making use of flux creep, which plays a relevant role at high temperatures.

Thanks to the extensive experimental campaign, the validity of a proposed scaling law applicable to REBCO tapes operated in a wide field, from zero up to 15 T, and temperature range, from 4.2 K up to T_c, has been confirmed. Fitting parameters for tapes procured from four different manufacturers have been derived. The scaling law is validated for tapes exposed to perpendicular magnetic fields.

ACKNOWLEDGEMENT

The authors would like to express their gratitude to Pierre-François Jacquot, Arnaud Vande Craen, Florian Girardot, Anne Eychenne and to the rest of the technical team of buildings 163 and 288 at CERN, for the invaluable technical support provided during the experimental campaign of tape testing.

REFERENCES

[1] J. Jiang *et al*., "High-performance Bi-2212 Round Wires Made With Recent Powders," *IEEE Trans. Appl. Supercond.*, vol. 29, no. 5, pp. 1-5, 2019, Art no. 6400405.

[2] National High Magnetic Field Laboratory website, https://nationalmaglab.org/magnet-development/applied-superconductivity-center/plots.

[3] S. R. Foltyn *et al., "*Material science challenges for high-temperature superconducting wire", *Nature Mater*., vol. 6, pp. 631-642, 2007.

[4] T. Puig, J. Gutierrez, X. Obradors, "Impact of high growth rates on the microstructure of high-temperature superconducting coated conductors", *Nature Reviews Physics*, vol. 6, pp. 132-148, 2024.

[5] C. Senatore *et al*., "Field and temperature scaling of the critical current density in commercial REBCO conductors", *Supercond. Sci. Techn.*, vol. 29, no. 1, 2016, Art. No. 014002.

[6] G. Succi, A. Ballarino, S. C. Hopkins, C. Barth, Y. Yang, "Magnetic field and temperature scaling of the critical current of REBCO tapes", *IEEE Trans. Appl. Supercond.*, vol. 34, no. 3, 2024, Art no. 8001007.

[7] E. J. Kramer, "Scaling laws for flux pinning in hard superconductors", *J. Appl. Phys.*, vol. 44, pp. 1360-1370, 1973.

[8] J. W. Ekin, "Unified scaling law for flux pinning in practical superconductors: I. Separability postulate, raw scaling data and parameterization at moderate strains", *Supercond. Sci. Technol*., vol. 23, no. 8, 2010, Art. No. 083001.

[9] N. Miura *et al*., "High-magnetic-field study of high-T_c cuprates", *Physica B*, vol. 319, pp. 310 – 320, 2002.

[10] T. Sekitani *et al*., "Upper critical field for optimally-doped $YBa_2Cu_3O_{7-\delta}$", *Physica B*, vol. 346 – 347, pp. 319-324, 2004.

[11] C. Xue *et al*., "Field-dependent critical state of high-T_c superconducting strip simultaneously exposed to transport current and perpendicular magnetic field", *AIP Advances* 3, 122110, 2013.

[12] A. Molodyk et al., "Development and large volume production of extremely high current density YBCO superconducting wires for fusion", *Sci. Rep*., vol. 11, 2021, Art. No. 2084.

[13] Y. Zhao *et al*., "Progress in fabrication of second generation high temperature superconducting tape at Shanghai Superconductor Technology", *Supercond. Sci. Techn.*, vol. 32, 2019, Art. No. 044004.

[14] A. Xu *et al*., "Strongly enhanced vortex pinning from 4 to 77 K in magnetic fields up to 31 T in 15 mol.% Zr-added (Gd, Y)-Ba-Cu-O superconducting tapes", *APL Mater. 2*, 046111, 2014.